SAN FRANCISCO ESTUARY & WATERSHED SCIENCE
Sponsored by the Delta Stewardship Council and UC Davis Institute of the Environment

RESEARCH

Climate Change Scenarios for Air and Water Temperatures in the Upper San Francisco Estuary: Implications for Thermal Regimes and Delta Smelt

Brock M. Huntsman[1*], Larry R. Brown[1], Marissa Wulff[1], Noah Knowles[2], R. Wayne Wagner[3], Frederick Feyrer[1]

ABSTRACT

Climate projections and their effects in the San Francisco Estuary have been evaluated as part of the US Geological Survey's CASCaDE2 project. Understanding the ecological effects of climate change can help manage and maintain the ecological health and productivity of the San Francisco Estuary. In this study, we assessed downscaled air temperature data from 10 global climate models (GCMs) under two representative concentration pathway (RCP) trajectories for greenhouse gas concentrations for three regions of the San Francisco Estuary: Sacramento–San Joaquin Delta, Suisun and Grizzly bays, and Suisun Marsh. We also used previously derived regression models to estimate future water temperatures at 16 locations in the upper San Francisco Estuary. We used a thermal regime approach to summarize water temperature projections to investigate changes to the thermal regime of the upper San Francisco Estuary, and used the Delta Smelt (*Hypomesus transpacificus*) to demonstrate the effects that a warming climate may have on the habitat needs of this fish species. Our results suggested there were no major differences in the extent of air-temperature warming among the three regions. Annual average air temperatures were projected to increase approximately 2.0 °C and 4.7 °C by the end of the century for the low and high RCP scenarios, respectively. We found timing, frequency, and magnitude metrics varied by period and RCP scenario, while duration and variability metrics varied by space for water-temperature thermal regimes. For example, the spawning window for Delta Smelt (thermal-regime duration metric) is projected to expand in the future, with spawning starting earlier for both RCP scenarios for most sites. Although our thermal-regime analysis focused on the life history of Delta Smelt, similar approaches could be used to assess climate-change threats to a wide array of native and invasive terrestrial and aquatic species found in San Francisco Estuary.

KEY WORDS

Sacramento River, San Joaquin River, Delta Smelt, CASCaDE2

SFEWS Volume 22 | Issue 2 | Article 1

https://doi.org/10.15447/sfews.2024v22iss2art1

* Corresponding author: bhuntsman@usgs.gov

1 California Water Science Center
US Geological Survey
Sacramento, CA 95819 USA

2 California Water Science Center
US Geological Survey
Menlo Park, CA 94025 USA

3 University of New Orleans
New Orleans, LA 70184 USA

INTRODUCTION

Climate change threatens many services that the San Francisco Estuary (the estuary) provides. For example, the upper estuary, which includes the Sacramento–San Joaquin Delta (Delta) and Suisun Bay (Figure 1), provides fresh water to many Californians. Projected sea level rise and increased salt intrusion into the upper estuary as a result of climate change have caused concern about the capacity of the upper estuary to supply fresh water in the future (Cloern et al. 2011; Bush et al. 2022; Herbold et al. 2022). Consequently, efforts by the California state legislature to meet the goals of providing a more reliable water supply for California—and to protect, restore, and enhance the Delta ecosystem—include promoting options for new and improved water-transport infrastructure (Sacramento–San Joaquin Delta Reform Act 2009). However, altered hydrodynamics is just one aspect of how climate change may affect the services the estuary provides.

Air and water temperatures are important to the ecological functioning of the estuary, and climate change is anticipated to considerably affect the ecosystem's thermal regime (see Cloern et al. 2011; Brown et al. 2013, 2016; Jeffries et al. 2016; Davis et al. 2019; Bashevkin et al. 2022; Bashevkin and Mahardja 2022). Like flow, temperature is a master variable that affects community dynamics of aquatic organisms (Olden and Naiman 2010; Arismendi et al. 2013). Temperature is a major driver of community structure and function because temperature controls physiological thresholds, food-web dynamics and productivity, and behavior of organisms (Brown et al. 2004; Daufresne et al. 2009; Sheridan and Bickford 2011; Armstrong and Schindler 2013; Cross et al. 2015). Thus, understanding current and future trends in temperatures in the upper estuary could aid development of proactive mitigation strategies to combat the potentially deleterious effects created by a changing climate.

Water-temperature patterns in the estuary are controlled by several factors, including atmospheric forcing, interacting effects of tides and rivers, water residence time, and heat and water exchange with groundwater. Air temperature is a major driver of water temperatures and ecosystem services and functions in the upper estuary (Kimmerer 2004; Wagner et al. 2011; Vroom et al. 2017). Contributions from other drivers vary predictably along a longitudinal gradient in the estuary, dominated by tides at western seaward locations and becoming more strongly affected by air temperature and riverine flow at more landward locations (Vroom et al. 2017).

Previous work on air temperature has focused on the entire Sacramento–San Joaquin Delta watershed (Knowles et al. 2018; Stern et al. 2020). Water-temperature models have previously been limited to a few emission scenarios derived from global climate models (GCMs; Cloern et al. 2011; Brown et al. 2013, 2016), or occur at a few fixed stations with long-term data availability (Wagner et al. 2011; Bashevkin et al. 2022; Bashevkin and Mahardja 2022). The goal of this study is to build on previous water-temperature modeling methods (Wagner et al. 2011) and available air-temperature projections for an ensemble of future scenarios (Pierce et al. 2014; Knowles et al. 2018; Wulff et al. 2021) to develop water-temperature projections at many locations in the estuary. To accomplish this goal, we have summarized projected air temperatures for three major regions of the upper estuary (Delta, Susuin and Grizzly bays, and Suisun Marsh; Figure 1). We have also updated projected water temperatures for 16 locations in the upper estuary using previously available regression equations (Wagner et al. 2011; Figure 1). We demonstrate the potential usefulness of these data using case studies to describe trends in air temperature, and by illustrating spatial and temporal changes in the thermal regime (Olden and Naiman 2010; Arismendi et al. 2013; Maheu et al. 2016) of water temperature based on climate projections. We describe thermal regimes in reference to the life-history requirements of the Delta Smelt (*Hypomesus transpacificus*), an endemic fish species listed as endangered under the California State Endangered Species Act and threatened under the Federal Endangered Species Act (CNDDB 2023).

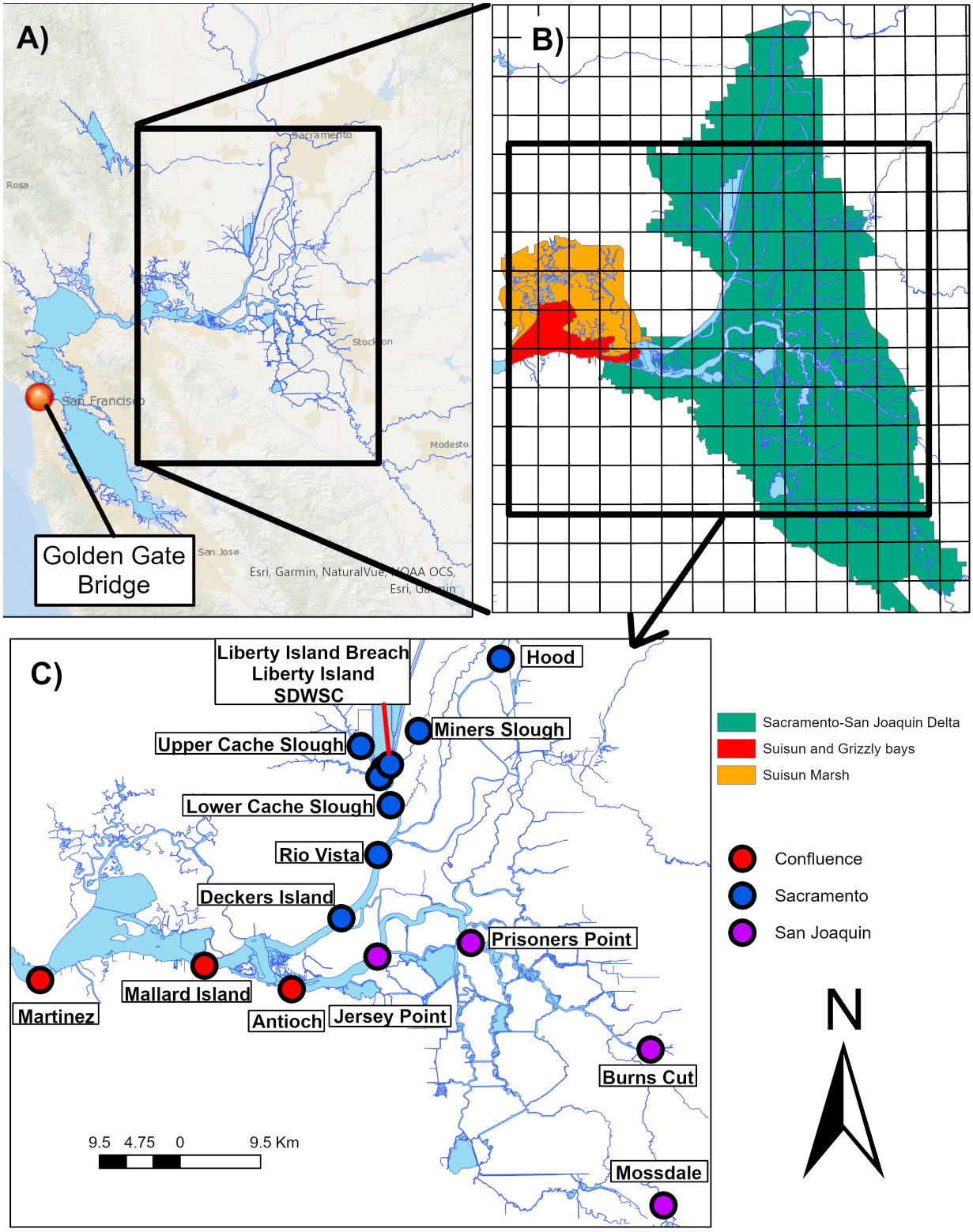

Figure 1 Site names of the 16 water-temperature sites used for water-temperature predictions in the San Francisco Estuary, California. (**A**) Grid cells for air-temperature projections in each region (**B**) and water-temperature sites (**C**) in the upper estuary are also provided. Symbol colors represent site locations in the Sacramento River, the San Joaquin River, or the confluence of both rivers.

https://doi.org/10.15447/sfews.2024v22iss2art1

METHODS

Data for this project were generated from the US Geological Survey CASCaDE2 project (Computational Assessments of Scenarios of Change for the Delta Ecosystem), which uses 20 Coupled Model Intercomparison Project Phase 5 (CMIP5) climate scenarios, consisting of 10 GCMs (Table 1) run with two representative concentration pathways (RCPs; Knowles et al. 2018). These two RCP pathways included the radiative forcing values of 4.5 and 8.5 W m^{-2} by the year 2100, which represent a scenario to abate greenhouse gas emissions (RCP 4.5) and a high-end emissions scenario (RCP 8.5). Further details on these scenarios can be found in Knowles et al. (2018).

Table 1 Global climate models (GCM) used for air- and water-temperature predictions in the San Francisco Estuary, California (*Source: Knowles et al. 2018; Stern et al. 2020*)

GCM	Modeling Center
ACCESS-1.0	Commonwealth Scientific and Industrial Research Organization and Bureau of Meteorology, Australia
CanESM2	Canadian Centre for Climate Modeling and Analysis
CCSM4	National Center for Atmospheric Research, USA
CESM1-BGC	National Science Foundation, Department of Energy, and National Center for Atmospheric Research, USA; Community Earth System Model
CMCC-CMS	Centro Euro-Mediterraneo per I Cambiamenti Climatici
CNRM-CM5	Centre National de Recherches Meteorologiques / Centre Europeen de Recherche et Formation Avancee en Calcul Scientifique, France
GFDL-CM3	National Oceanic and Atmospheric Administration Geophysical Fluid Dynamics Laboratory, USA
HadGEM2-CC	Met Office Hadley Centre, United Kingdom
HadGEM2-ES	Met Office Hadley Centre (Additional realizations), United Kingdom
MIROC5	Atmosphere and Ocean Research Institute, National Institute for Environmental Studies, and Japan Agency for Marine-Earth Science and Technology

Air Temperature

We generated GCM-derived air temperatures for each of the 20 climate scenarios for 1980–2099 at daily time increments on a one-sixteenth-degree grid (Pierce et al. 2014). We constrained GCM projections to 2099 instead of 2100 because some GCM projections end in 2099. We calculated daily average air temperatures for three regions of the upper estuary: the Delta, Suisun and Grizzly bays, and Suisun Marsh (Figure 1B). Additionally, we used an observation-based dataset on the same one-sixteenth-degree grid (Livneh et al. 2015) to provide a historical baseline from 1980–2009 to compare with GCM-derived climate scenarios (Knowles et al. 2018). The dataset included daily minimum and daily maximum near-surface air temperatures, and we calculated daily average values from these daily minimums and daily maximums.

We summarized daily air-temperature metrics (daily averages, minimums, and maximums) among the three regions of the upper estuary (Delta, Suisun and Grizzy bays, and Suisun Marsh) for each climate scenario by water year (the period from October 1 through September 30; e.g., water year 2012 is October 1, 2011 through September 30, 2012) as monthly and annual average temperatures. We estimated the magnitude of temperature change for each of the three air-temperature metrics summarized by period (i.e., each month and annually) for each climate scenario and each region using Sen's slope estimator, which is a non-parametric test that represents the median slope of all pairs in the dataset (Sen 1968; Arismendi et al. 2013). For simplicity, we summarized each future air temperature metric (2010–2099) for all GCMs into an ensemble mean for the 4.5 emission scenario and an ensemble mean for the 8.5 emission scenario (means among all GCMs). Lastly, we estimated the magnitude of change with Sen's slope estimator for each air-temperature metric summarized by period and region during baseline conditions (1980–2009) using observations from Livneh et al. (2015).

Water Temperature

We modeled daily water temperatures at 16 monitoring sites in the upper estuary based on

previously established regression equations (Wagner et al. 2011, *http://www.iep.ca.gov*; Figure 1). We report only daily average values for water temperature from this point forward, but modeled daily minimum and maximum temperature values are available in Wulff et al. (2021). Wagner et al. (2011) developed predictive regression equations for water temperature at these 16 sites of the upper estuary as a function of air temperature and insolation (R, a measure of the amount of the sun's energy reaching earth) on the same day (i), and the preceding day's daily average water temperature (W_{i-1}):

$$W_i = \alpha A_i + \beta W_{i\text{-}1} + \gamma R_i + \tau \qquad \text{Eq 1}$$

where α, β, γ, and τ are regression coefficients for the daily average air temperature, previous day's daily average water temperature, insolation effect, and a constant offset, respectively (Table A1). We downloaded insolation data from the California Irrigation Management Information System (CDWR 2020) for seven locations in the upper estuary (Lodi, Brentwood, Manteca, Twitchell Island, Lodi West, Tracy, and Concord; see Wagner et al. 2011 for more detail), and we used the average value (arithmetic mean) among locations for each day for all water-temperature predictions as recommended by Wagner et al. (2011). We used historical air temperatures (1980–2009, Livneh et al. 2015) and projected air temperatures for both RCPs of each GCM that were made available by the CASCaDE2 project (Knowles et al. 2018) to expand Wagner et al.'s (2011) water-temperature predictions from two to 10 GCMs (see Brown et al. 2016). We used projected air-temperature data downscaled to a 12-km grid for the upper estuary and averaged among grid cells to develop our water-temperature regression models based on Equation 1.

We explored spatial and temporal patterns in baseline and forecasted water temperatures using a thermal-regime analytical framework (Olden and Naiman 2010; Arismendi et al. 2013; Isaak et al. 2020). We summarized time-series of daily average water temperatures for each water year into metrics that were organized into five discrete thermal-regime categories (magnitude, frequency, timing, duration, and variability; Table 2, Figure 2; Arismendi et al. 2013)—metrics associated with spring (March–May), summer (June–August), fall (September–November), and winter (December–February) months. We used

Table 2 Definition of thermal-regime metrics used for water temperature at 16 locations in the San Francisco Estuary, California

Thermal regime	Metric	Units	Definition
Magnitude	MWMT	°C	Maximum weekly maximum temperature estimated as the maximum of the 7-day moving average of the maximum daily temperature.
	MWAT	°C	Maximum weekly average temperature estimated as the maximum of the 7-daily moving average of the mean daily temperature.
	Degree-Days	°C	Accumulation of temperature over time.
Variability	MeanRange	°C	Difference between the highest and lowest daily mean temperature.
	MaxRange	°C	Difference between the highest and lowest maximum daily temperature.
	CVmax	None	Coefficient of variation among daily maximum temperatures.
	CVmean	None	Coefficient of variation among daily mean temperatures.
Timing	CTD50	Day	Date of attaining 50% of the degree days for a year.
	CTD75	Day	Date of attaining 75% of the degree days for a year.
	SpawnMedian	Day	Median date of the spawning window for Delta Smelt (See SpawnDays).
	SpawnStart	Day	Start of the spawning window for Delta Smelt, initiated after 5 consecutive days at or above 15 °C following the first of February each year (See SpawnDays).
Duration	SpawnDays	Number of days	Number of days within the spawning window for Delta Smelt. The spawning window starts after 5 consecutive days at or above 15 °C following the first of February and ends after 5 consecutive days at or above 20 °C.
Frequency	AboveThreshold	Number of days	Number of days that exceed the acute lethal temperature for Delta Smelt, 25 °C.

https://doi.org/10.15447/sfews.2024v22iss2art1

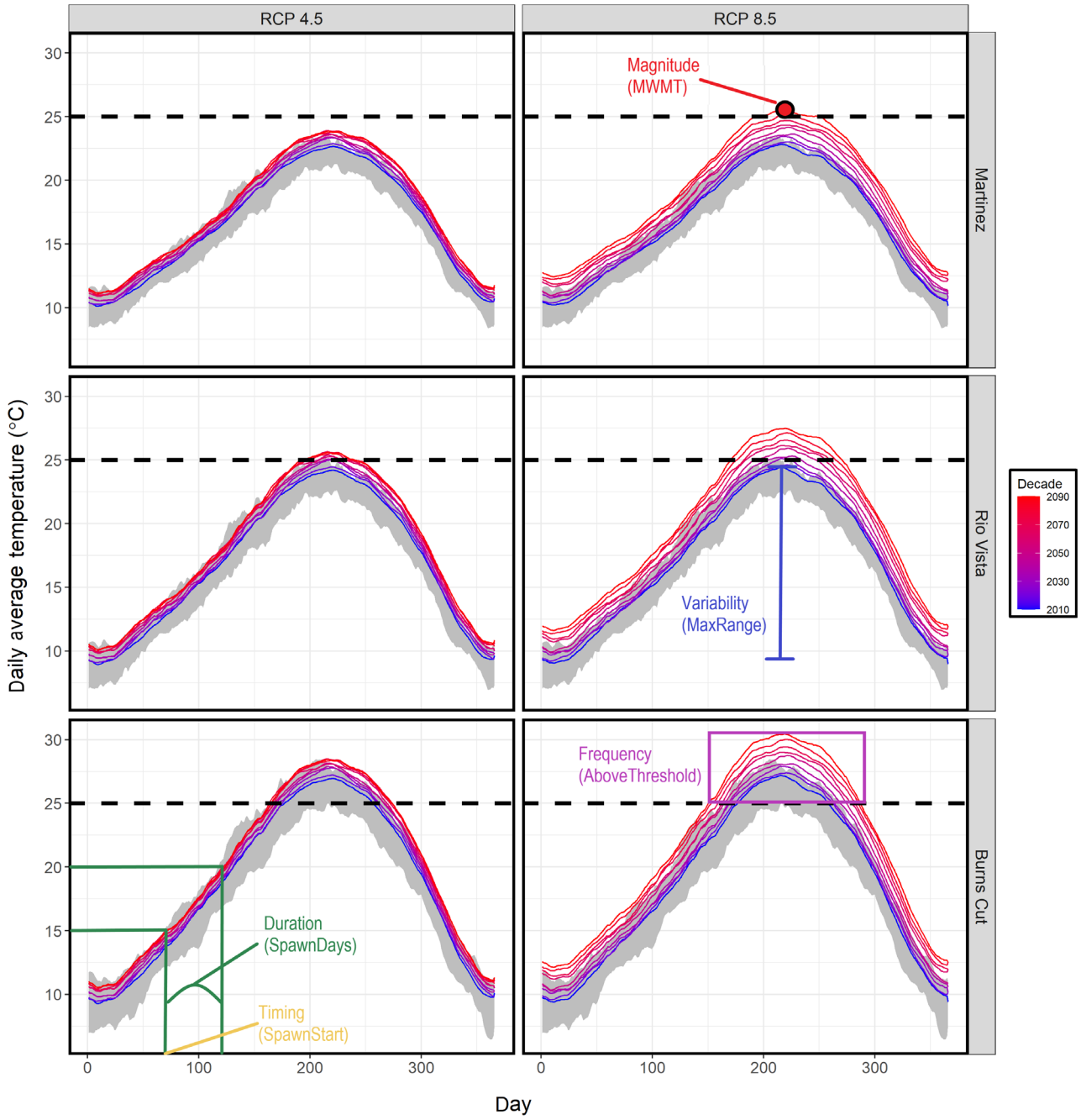

Figure 2 Predicted daily average water temperatures at three sites under the RCP 4.5 and RCP 8.5 ensemble scenarios in the San Francisco Estuary, California. The *gray polygon* represents the daily average minimum and daily average maximum predicted water temperatures for each day during the historical record (1980–2009). *Individual lines* are summarized mean temperatures by decade (2010–2019, 2020–2039, etc.).

similar definitions for thermal-regime metrics as described by Olden and Naiman (2010) for this study, where thermal regimes describe the magnitude of water temperatures, frequency of occurrence of a given temperature, the time at which a given temperature occurs (day), the duration of time in which a given temperature occurs (number of days), and how quickly a temperature metric changes or how variable that metric is over a period of days.

We focused on calculating thermal-regime metrics relative to physiological thresholds relevant to important life-history events for Delta Smelt (*Hypomesus transpacificus*), a pelagic fish native to the estuary that has been the focus of much conservation effort (Brown et al. 2013, 2016; Table 2). The spawning window of Delta Smelt was defined as the date when water temperatures reached 15 °C during spring months for 5 consecutive days and ends when temperatures exceed 20 °C for 5 consecutive days (Bennett 2005; Brown et al. 2016). The spawning window was used to define thermal-regime metrics specific to timing (start, median, and end of the spawning window based on date), and the duration of the spawning window (total number of days in the window). We also calculated a metric for the number of days above the acute lethal thermal limit for Delta Smelt (25 °C) as described by Brown et al. (2013). All other metrics used to describe the thermal regime of the upper estuary are defined in Table 2.

We used non-metric multidimensional scaling (nMDS) ordination in program R (Oksanen et al. 2020; R Core Team 2021) to describe how the thermal regime among locations in the upper estuary may change under various climate scenarios (baseline, RCP 4.5, RCP 8.5). We estimated the magnitude of change in each thermal-regime metric among all locations using the Sen's slope estimator from the "trend" package (Pohlert 2020) in program R, similar to methods described for air-temperature analyses. Lastly, we used the Sen's slope estimator to describe the magnitude of change for monthly average water temperature (average of daily average temperatures for a month) and annual average water temperature (average of daily average temperatures for a full year), similar to our air-temperature analysis.

RESULTS

Air Temperature

Trends in air-temperature metrics (daily minimum, average, and maximum) either increased or decreased based on temperature summaries at monthly or annual time-scales under historical baseline conditions (1980–2009). Annual average air temperatures for baseline conditions increased for all three regions (Delta, Suisun and Grizzly bays, and Suisun Marsh; Table 3), with annual average air temperatures increasing by 0.025 °C per year for the Suisun and Grizzly bays and Suisun Marsh, and by 0.021 °C per year for the Delta (Figure 3; Table 3). Monthly average air temperatures for baseline conditions demonstrated an increasing trend for all months and regions except that monthly average temperatures (1) decreased in the Delta during May (–0.011 °C per year) and July (–0.015 °C per year), (2) decreased in Suisun and Grizzly bays during December (–0.003 °C per year), and (3) decreased in Suisun Marsh during July (–0.003 °C per year) and December (–0.002 °C per year; Table 3). Similar decreasing trends in air temperature were observed for monthly average minimum and maximum temperatures during May and July for the Delta (Table 3). However, monthly average maximum temperatures decreased in May and July through November in Suisun and Grizzly bays and in Suisun Marsh (Table 3). Lastly, monthly average maximum temperatures also decreased during March in Suisun Marsh (–0.007 °C per year; Table 3).

Unlike historical baseline conditions, all monthly and annual temperature metrics for future emission scenarios increased (Table 3). Consequently, we only describe patterns in daily average air-temperature metrics for simplicity from this point forward. Sen's slope estimates indicated that the magnitude of warming air temperatures was lowest during the summer months (June–August Sen's slopes = 0.009–0.017 °C per year among regions), while late fall and early winter months (October, November, and December) demonstrated the highest air-temperature warming trends for the RCP 4.5 emission scenarios (Table 3; Sen's slope = 0.028–0.032 °C per year among regions). Similar warming trends by month were observed for the RCP 8.5 emission scenarios, although the Sen's slope indicated a greater magnitude in change (summer months Sen's slope = 0.032–0.042 °C per year, late fall and early winter months Sen's slope = 0.063–0.075 °C per year; Table 3).

https://doi.org/10.15447/sfews.2024v22iss2art1

Table 3 Trend analysis for daily air temperature metrics under baseline, RCP 4.5, and RCP 8.5 ensemble scenarios in the San Francisco Estuary, California. Values are the Sen's slope (°C per year). Period represents monthly and annual average air–temperature metrics for each location.

		Baseline			RCP 4.5			RCP 8.5		
Location	**Period**	**Minimum**	**Mean**	**Maximum**	**Minimum**	**Mean**	**Maximum**	**Minimum**	**Mean**	**Maximum**
Sacramento–San Joaquin Delta	Jan	0.005	0.009	0.005	0.026	0.024	0.027	0.055	0.054	0.057
	Feb	0.053	0.045	0.055	0.023	0.020	0.026	0.056	0.050	0.061
	Mar	0.012	0.008	0.013	0.019	0.017	0.022	0.045	0.042	0.047
	Apr	0.031	0.044	0.027	0.020	0.022	0.018	0.044	0.042	0.045
	May	−0.029	−0.011	−0.035	0.022	0.021	0.024	0.041	0.041	0.040
	Jun	0.048	0.018	0.076	0.018	0.017	0.019	0.038	0.035	0.039
	Jul	−0.013	−0.015	−0.017	0.016	0.013	0.018	0.041	0.036	0.046
	Aug	0.034	0.038	0.039	0.021	0.016	0.024	0.049	0.041	0.057
	Sep	0.025	0.021	0.034	0.029	0.024	0.034	0.059	0.055	0.064
	Oct	0.046	0.041	0.046	0.030	0.029	0.032	0.061	0.063	0.058
	Nov	0.039	0.050	0.031	0.028	0.028	0.027	0.066	0.070	0.062
	Dec	0.055	0.035	0.063	0.032	0.031	0.032	0.068	0.069	0.066
	Annual	0.026	0.021	0.026	0.024	0.022	0.025	0.052	0.050	0.054
Suisun and Grizzly bays	Jan	0.000	0.005	0.007	0.028	0.026	0.028	0.058	0.056	0.059
	Feb	0.064	0.060	0.060	0.021	0.018	0.024	0.053	0.047	0.060
	Mar	0.008	0.016	0.001	0.020	0.017	0.022	0.046	0.043	0.048
	Apr	0.024	0.031	0.012	0.022	0.024	0.019	0.047	0.046	0.048
	May	−0.021	0.011	−0.040	0.025	0.024	0.027	0.046	0.047	0.046
	Jun	0.044	0.014	0.072	0.015	0.014	0.017	0.034	0.032	0.035
	Jul	−0.021	0.000	−0.011	0.012	0.010	0.014	0.039	0.033	0.043
	Aug	0.036	0.037	−0.002	0.020	0.016	0.023	0.050	0.042	0.058
	Sep	0.013	0.036	−0.014	0.030	0.026	0.034	0.063	0.059	0.067
	Oct	0.006	0.030	−0.013	0.032	0.031	0.034	0.065	0.068	0.062
	Nov	0.011	0.033	−0.012	0.032	0.032	0.031	0.070	0.075	0.066
	Dec	0.018	−0.003	0.026	0.033	0.032	0.033	0.067	0.069	0.065
	Annual	0.017	0.025	0.009	0.024	0.022	0.026	0.053	0.052	0.055
Suisun Marsh	Jan	0.000	0.001	0.008	0.027	0.025	0.027	0.057	0.055	0.058
	Feb	0.062	0.064	0.055	0.021	0.017	0.024	0.053	0.046	0.059
	Mar	0.007	0.018	−0.007	0.019	0.017	0.022	0.045	0.042	0.047
	Apr	0.025	0.034	0.013	0.022	0.024	0.019	0.047	0.046	0.047
	May	−0.019	0.014	−0.040	0.025	0.024	0.026	0.046	0.046	0.045
	Jun	0.045	0.012	0.072	0.015	0.014	0.017	0.034	0.032	0.035
	Jul	−0.023	−0.003	−0.011	0.012	0.009	0.014	0.039	0.033	0.043
	Aug	0.030	0.034	−0.002	0.020	0.015	0.023	0.049	0.042	0.057
	Sep	0.008	0.032	−0.016	0.029	0.025	0.034	0.063	0.059	0.066
	Oct	0.001	0.024	−0.017	0.032	0.031	0.034	0.065	0.068	0.062
	Nov	0.006	0.030	−0.012	0.032	0.032	0.031	0.070	0.075	0.066
	Dec	0.019	−0.002	0.033	0.033	0.032	0.033	0.067	0.069	0.065
	Annual	0.017	0.025	0.006	0.024	0.022	0.025	0.053	0.051	0.054

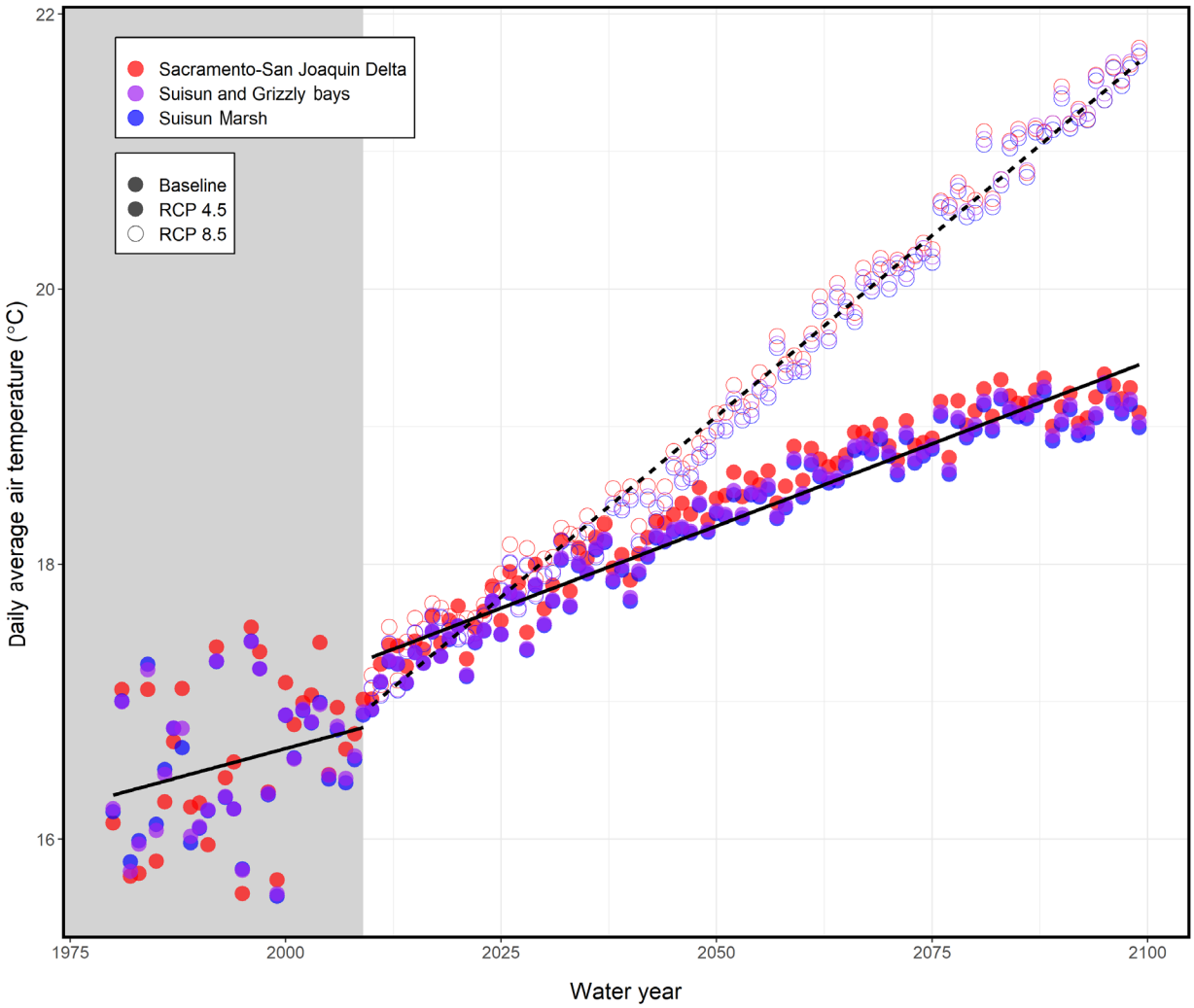

Figure 3 Predicted daily average air temperature for three regions of the San Francisco Estuary, California, during baseline historical conditions (before 2010) and projected under two emission scenarios (RCP 4.5 and RCP 8.5).

Water Temperature

Water temperatures under baseline and future emission scenarios varied by month and location in the upper estuary (Figure 4). Temperatures were consistently warmest in the San Joaquin River water-temperature sites (Burns Cut, Mossdale, and Prisoners Point sites), intermediate in the Sacramento River water-temperature sites (Hood, Miners Slough, and lower and upper Cache Slough sites), and coolest in the confluence water-temperature sites (Martinez, Mallard Island sites) during all but the winter months (December–February; Figure 1). For example, the Burns Cut (26.2 °C), Mossdale (25.6 °C), and Prisoners Point (24.4 °C) sites had the three warmest monthly average water temperatures predicted for July under baseline conditions (Figure 4), while three of the four warmest sites predicted for January were sites near the confluence of the San Joaquin and Sacramento rivers (Martinez = 10.5 °C, Antioch = 10.4 °C, Mallard Island = 10.2 °C; Figure 4). Most sites in the Sacramento River were predicted to be relatively cool compared to sites in the San Joaquin River at similar distances from the Golden Gate Bridge for nearly all months and were slightly warmer than sites downstream of the confluence (Martinez and Mallard Island; Figure 4).

https://doi.org/10.15447/sfews.2024v22iss2art1

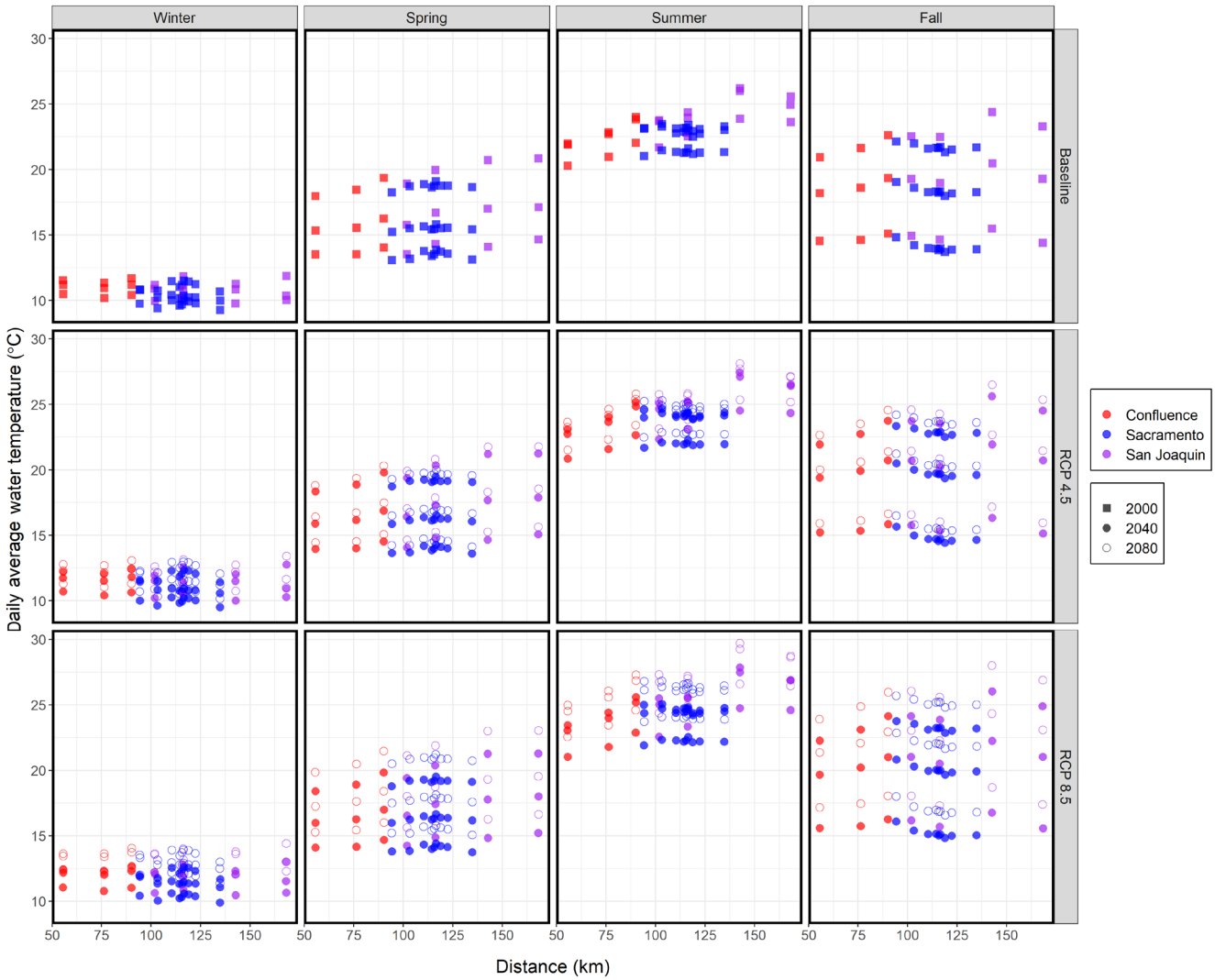

Figure 4 Predicted daily average water temperature by season and distance (km) from the Golden Gate Bridge (see Figure 1) for 2000, 2040, and 2080 under the baseline and ensemble RCP 4.5 and RCP 8.5 scenarios for 16 sites in the San Francisco Estuary, California. Each season has *three points*: one for each month of that season (summer = June through August, fall = September through November, winter = December through February, and spring = March through May). *Colors* represent the location of a site, being the Sacramento River, San Joaquin River, or the confluence of both rivers (see Figure 1).

Trend analysis of monthly and annual average water temperatures demonstrated differences between baseline conditions (1980–2009) and future scenarios (RCP 4.5 and 8.5, 2010–2099). Similar to trends in air temperature, monthly and annual average water temperatures demonstrated an increasing trend in temperature for RCP 4.5 emission scenarios and a greater magnitude in increasing temperature trends for the RCP 8.5 emission scenarios based on Sen's slope values (Table A2).

Non-metric multidimensional scaling ordination of thermal-regime metrics converged in two dimensions with a stress of 0.08, indicating strong separation among thermal-regime metrics in two dimensions (Figure 5). Thermal-regime metrics separated along obvious gradients in two-dimensional (2-D) space, with more seaward sites depicted at the negative end of MDS 1 and 2 and more landward sites found on the positive end of both MDS axes (Figure 5C). An opposite pattern in thermal-regime metrics was observed in 2-D space along a temporal gradient, with baseline

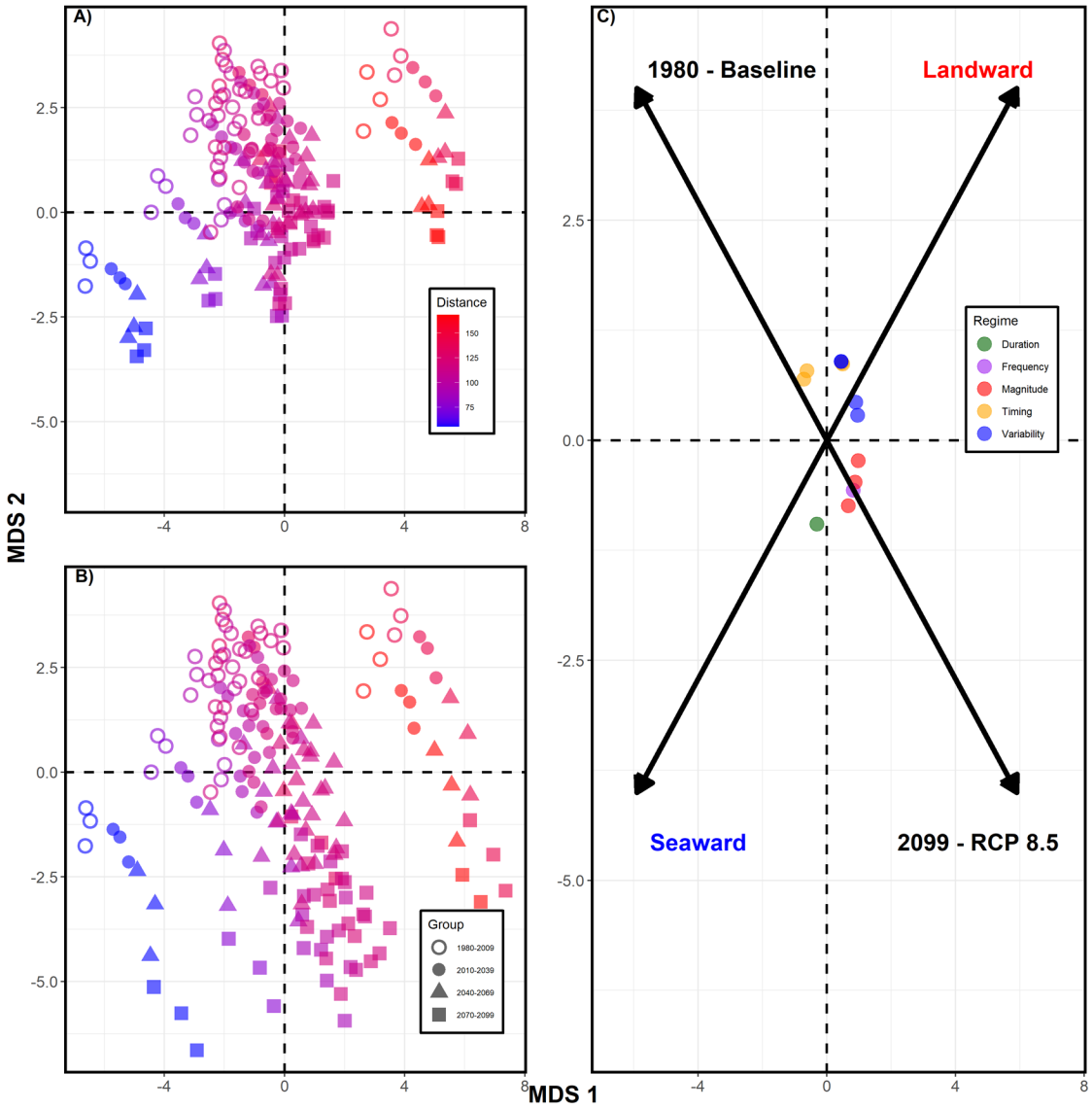

Figure 5 Non-metric multidimensional scaling plot of water-temperature metrics (see Table 3) representing the thermal regime of the San Francisco Estuary, California. Calculated metrics are summarized at 30-year intervals for the historical baseline conditions (1980–2009, open symbols), and the (**A**) RCP 4.5 and (**B**) RCP 8.5 emission scenarios. The general spatial and temporal pattern in the thermal regime is summarized in biplot space for MDS 1 and 2 in panel (**C**). Distance represents the in-water distance (km) a location was from the Golden Gate Bridge.

conditions found in the top-left corner of the biplot space (negative MDS 1 and positive MDS 2) and future conditions (2099) under the highest RCP emission scenarios found in the bottom-right corner of biplot space (positive MSD 1 and negative MDS 2; Figure 5C). Thermal-regime metrics in biplot space indicated that metrics representing magnitude of the thermal regime more strongly loaded on the bottom-right of the nMDS biplot, where future conditions at the highest emission scenarios also loaded (Figure 5). Thermal-regime metrics that represented variability loaded more strongly on the positive end of MDS 1 and MDS 2 of biplot space, where more landward sites loaded (Figure 5). Thermal-regime metrics that represented timing loaded more strongly on the negative side of MDS 1 and positive side of MDS 2 in biplot space, where baseline conditions were located. Lastly, thermal-regime metrics that represented duration more

https://doi.org/10.15447/sfews.2024v22iss2art1

strongly loaded on the negative side of MDS 1 with conditions found at more seaward locations (Figure 5).

Trend analysis of thermal-regime metrics during baseline conditions demonstrated greater variability in Sen's slope estimates among sites than for future scenarios (Figure 6). Magnitude thermal-regime metrics increased for most sites with a general pattern of a decreasing trend for all other thermal-regime metrics during baseline conditions (Figure 6). Trend analysis indicated that under future emission scenarios, metrics used to describe the magnitude, duration, and frequency of the upper estuary's thermal regime increased, timing metrics decreased, and variability metrics showed no discernable patterns (Figure 6).

The number of days above the acute lethal temperature limit for Delta Smelt of 25 °C increased for all sites. The magnitude of increase was lowest at the Martinez site (Sen's slope = 0.04 days per year for RCP 4.5 emission scenarios and 0.43 days per year for RCP 8.5 emission scenarios) and highest at the Jersey Point site (Sen's slope = 0.64 days per year for RCP 4.5 emission scenarios and 1.20 days per year for RCP 8.5 emission scenarios; Table A2). The timing in which spawning would occur was predicted to start earlier under all future scenarios at all sites (SpawnStart, SpawnMedian), and the duration of the spawning window was predicted to increase for all sites and future emission scenarios other than at the lower Cache Slough and the Sacramento River Deep Water Ship Channel (SDWSC) sites (Figure 7).

DISCUSSION

We observed warming trends for air- and water-temperature metrics that were similar to results of previous studies (Cloern et al. 2011; Wagner et al. 2011; Brown et al. 2013, 2016). We built on those results by generating information from a greater number of GCMs with more recent greenhouse gas emission scenarios to provide more robust projections, which may help guide restoration efforts in response to a changing climate (Palmer et al. 2009; Cloern et al. 2011).

Temperature Change in the Estuary

Air-temperature projections from downscaled GCMs for the three regions of the upper estuary (Delta, Suisun and Grizzy bays, and Suisun Marsh) showed little spatial variability under current and projected climate scenarios, which may be a result of the close proximity of these regions to one another and their similar topography. Cayan et al. (2008) showed that air temperatures in California are projected to warm approximately 1.5 °C under low-emission scenarios and as high as 4.5 °C under high- emission scenarios by 2100. We found similar air-temperature trends among the three regions of the upper estuary where mean daily average air temperatures are projected to increase approximately 2 °C under the low-emission scenarios (RCP 4.5) and approximately 4.5 °C under the high-emission scenarios (RCP 8.5) by the end of the century. Our air-temperature values were downscaled to finer spatial scales but were all within the same climate zone of California (zone 12; Sherbakov et al. 2018).

Seasonal patterns in projected water temperatures were more spatially variable than seasonal patterns in air temperatures. Monthly average water temperatures were warmest during winter months at more seaward sites and warmest during summer months at the more landward sites, specifically in the San Joaquin River watershed. These observed spatial and seasonal patterns in water temperatures in the upper estuary are consistent with expectations that effects of air temperature and riverine inputs increase with increases in distance from marine inputs (Vroom et al. 2017). Additionally, projected water temperatures during summer months were higher at sites in the San Joaquin River watershed than in the Sacramento River watershed, a pattern that may be influenced by outflow-temperature relationships. Kimmerer (2004) showed that the correlation between air and water temperatures weakened during high flows, but this relationship was stronger in the Sacramento River upstream of the confluence of the Sacramento and San Joaquin rivers (at Freeport, which is upstream of

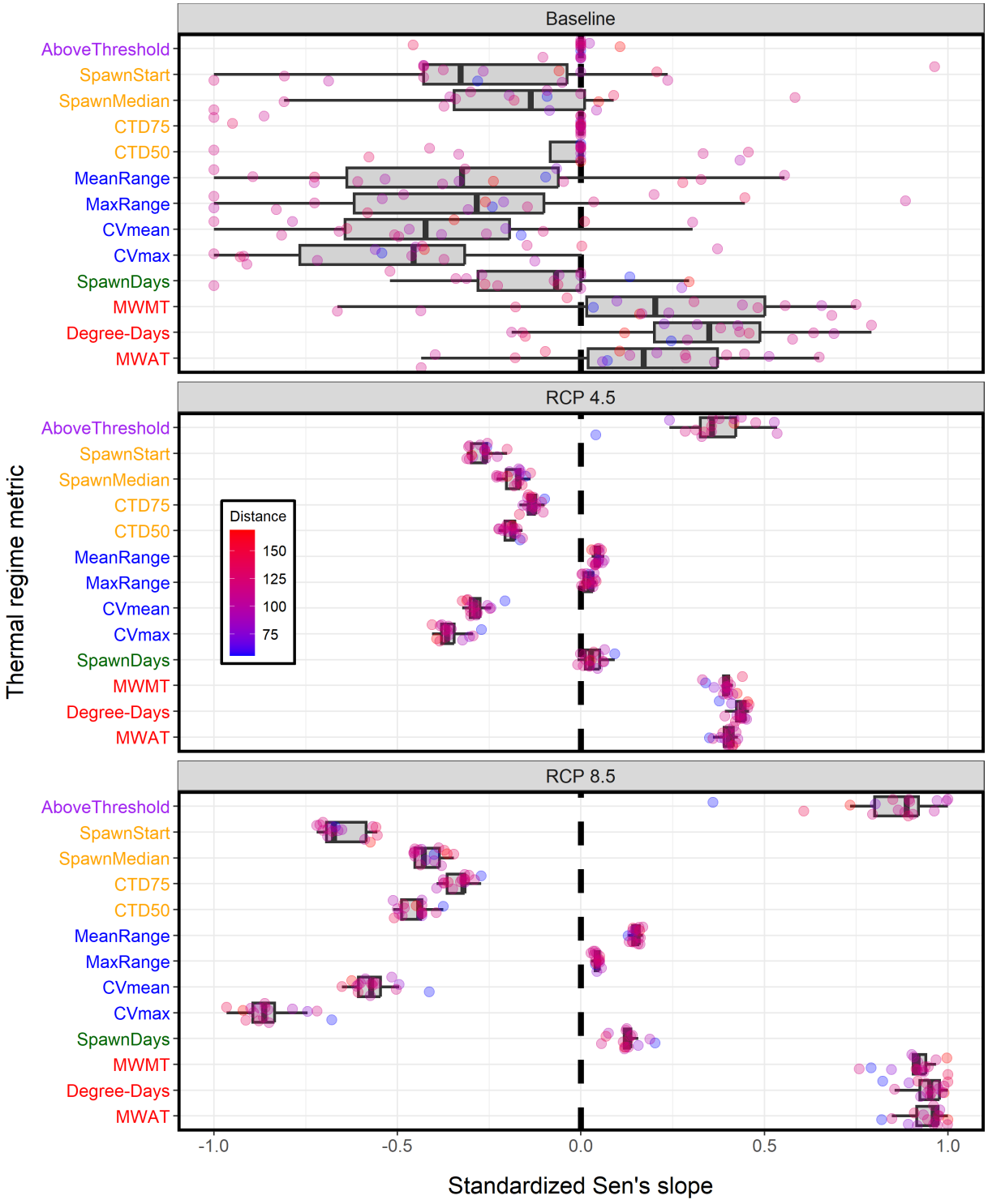

Figure 6 Trends (standardized Sen's slope) in thermal-regime metrics under historical conditions and two emission scenarios (RCP 4.5 and RCP 8.5) for stations in the San Francisco Estuary, California. *Color gradients* represent in-water distance (km) of a location from the Golden Gate Bridge, with the stations closest to marine influence represented by cool colors. Colors of each metric on the *y*-axis indicates to which thermal-regime category a metric belongs. *Red* metrics represent Magnitude, *green* = Duration, *blue* = Variability, *orange* = Timing, and *purple* = Frequency. The Sen's slope for each metric was standardized by dividing the site-specific estimate by the largest absolute value.

https://doi.org/10.15447/sfews.2024v22iss2art1

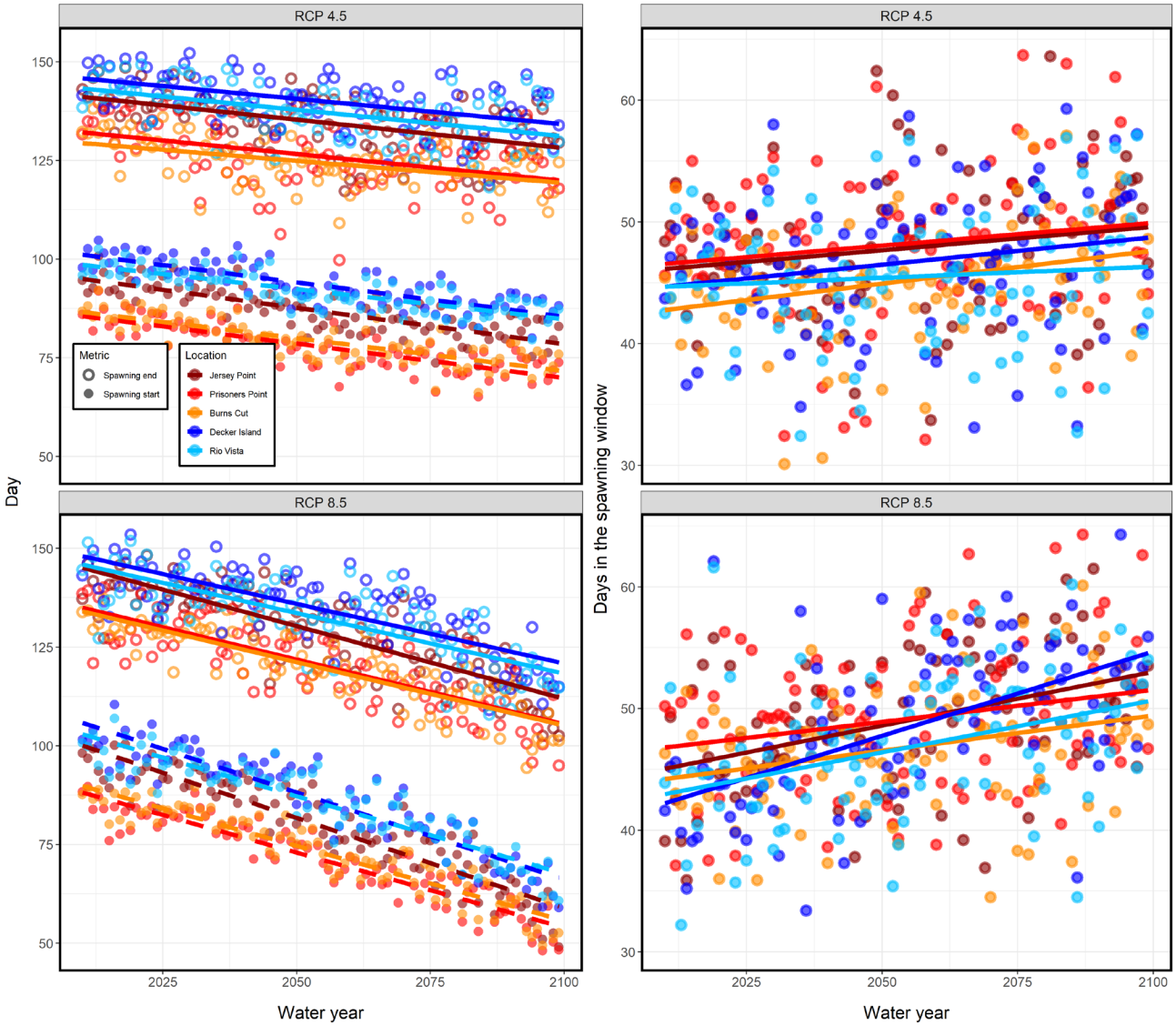

Figure 7 Trends in the starting and ending day of a Delta Smelt's spawning window estimated for four locations in the San Francisco Estuary, California. Each *point* is a GCM ensemble estimate for either the RCP 4.5 or RCP 8.5 emission scenario.

Hood) compared to near Antioch. The Sacramento River contributes approximately 85% of inflow to the upper estuary compared to the San Joaquin River's approximately 11%; thus, warmer water at sites in the smaller San Joaquin River may demonstrate that water temperatures equilibrate faster with air temperatures during warmer months in less water (Kimmerer 2004; Bashevkin et al. 2022).

Climate Change Effects on Delta Smelt in the Upper Estuary

Our results demonstrate that a changing climate is projected to spatially and temporally alter the upper estuary's thermal regime. Spatially, we found that metrics representing variability and duration in the thermal regime distinguished sites at more landward locations from sites at more seaward locations near the Sacramento–San Joaquin confluence. These spatial patterns in the thermal regime are not surprising because water temperature in the upper estuary is closely linked

to more variable air temperatures landward and the influence of less-variable ocean temperatures at more seaward locations (Kimmerer et al. 2004). Metrics that represented timing, magnitude, and frequency varied by emission scenarios and temporally (by year), having implications for future Delta Smelt life-history events (e.g., spawning) and demography (e.g., temperatures that exceed critical thresholds).

Projected water temperatures in the upper estuary indicate that the spawning window for Delta Smelt may expand in the future. We found earlier starting and ending dates for spawning at most sites for both RCP emission scenarios, but the trend was stronger for starting dates than for ending dates. Bashevkin and Mahardja (2022) found that historical water temperature trends in the upper estuary varied spatially, and the strength of trends depended on season. Specifically, Bashevkin and Mahardja (2022) found that warming trends in the upper estuary were strongest during winter months (November–February). Consequently, warmer temperatures in late winter would allow for spawning to occur earlier in the year, and the weaker warming signal for early spring results in similar dates at which spawning ends. We found evidence for warming trends for all months and sites under the RCP 8.5 emission scenarios. However, warming trends during early spring months (March = 0.024–0.030 °C per year, April = 0.028–0.034 °C per year) were slightly weaker than during the winter months (December = 0.031–0.038 °C per year, January = 0.029–0.035 °C per year), providing some evidence for stronger warming trends during future winter months than during spring months. The warming temperatures may expand the spawning window of Delta Smelt, potentially benefitting their recruitment process as long as other aspects of their early life-history are not affected (e.g., match–mismatch hypothesis; Merz et al. 2016).

One caveat to consider when interpreting the patterns in spawning windows of Delta Smelt observed in this study is that temperature is not the only factor that influences spawning behavior or spawning success. For example, early winter flows play an important role in triggering the upstream (landward movement toward freshwater spawning habitat) spawning movements of Delta Smelt (Sommer et al. 2011). Consequently, an earlier and expanded spawning window from a projected future climate in the upper estuary may not result in expanded spawning investment by Delta Smelt if elevated flows do not trigger upstream spawning movements. Climate scenarios project highly variable future precipitation patterns in the Central Valley of California, with conditions anticipated to result in more frequent and severe dry years (Knowles et al. 2018; Stern et al. 2020). Furthermore, an earlier spawning window would result in fewer days for somatic growth and gamete production, potentially resulting in lower per capita fecundity from smaller Delta Smelt (Damon et al. 2016). Lastly, the distribution of Delta Smelt throughout the year would be important to consider in the context of thermal-regime metrics like the spawning window, where metrics that represent life-history events such as spawning would be most valuable if calculated in areas where these events most commonly occur in the upper estuary (more landward than seaward; Merz et al. 2011).

The Delta Smelt is currently managed as a semi-anadromous species for which reproduction occurs in freshwater spawning areas during spring months, and more seaward habitat downstream of the Sacramento–San Joaquin confluence is accessed as foraging habitat later in the year (Moyle et al. 2016). However, Hobbs et al. (2019) recently showed that three life-history phenotypes exist in Delta Smelt: a freshwater resident, brackish water resident, and semi-anadromous. Consequently, water temperatures in the freshwater extent of the upper estuary indicate that the year-round freshwater strategy may not be viable for future populations. For example, our results indicate that the number of days exceeding the acute lethal temperature for Delta Smelt (25 °C; Brown et al. 2013) is projected to be greater than 3 months in the San Joaquin River and greater than 2 months in the Sacramento River (upstream of the confluence of the Sacramento and San Joaquin rivers) by 2080 under the high-emission scenario (RCP 8.5). Based

https://doi.org/10.15447/sfews.2024v22iss2art1

on our current knowledge of Delta Smelt life-history strategies (freshwater resident strategy; Hobbs et al. 2019), 12% of the population would be lost if suitable freshwater habitat could not be accessed year-round because of a warming climate.

Climate change literature supports three universal responses by ectotherms to a warming climate. Ectotherms can (1) show an altitudinal/latitudinal shift in distributions, (2) adopt a phenological response, or (3) become smaller in size (Daufresne et al. 2009; Sheridan and Bickford 2011). Evidence for phenological shifts (Merz et al. 2016; Munsch et al. 2019; Goertler et al. 2021) have already been documented for organisms found in the upper estuary, and we have shown that the timing of Delta Smelt spawning in the future is projected to start earlier throughout most of the upper estuary based purely on temperature cues (e.g., other factors, such as flow, are believed to play a role in Delta Smelt spawning behavior; Sommer et al. 2011). Altitudinal/latitudinal shifts are less relevant if considered within the upper estuary boundary, but longitudinal shifts may be important as cooler and more stable temperatures are predicted for locations at more western regions of the upper estuary as a result of greater marine influence on temperatures.

Salinity is also projected to increase in the upper estuary because climate models project rising sea levels and reduced dry-season freshwater outflow—two factors that control salt intrusion into the upper estuary (Cloern et al. 2011; Bush et al. 2022). Delta Smelt are relatively resilient to elevated salinities (Komoroske et al. 2014; Kammerer et al. 2016; Hung et al. 2022), suggesting that more seaward habitat may provide the most hospitable habitat in the future. However, the energetic costs associated with enduring elevated salinities and temperatures may have compounding sub-lethal effects on Delta Smelt populations, such as poorer condition, slower growth, and reduced fecundity (Ghalambor et al. 2021). Potential sub-lethal effects of increased salinities and temperatures were not examined in this study, but improved understanding of sub-lethal effects could further inform management strategies to maintain populations of Delta Smelt in the upper estuary as climate changes.

The metabolic theory of ecology predicts shrinking ectotherm body size with increasing temperatures because body size and temperature affect the metabolic rate of ectotherms (Brown et al. 2004). Evidence for shrinking body sizes in the upper estuary with warming temperatures has been limited to invertebrate communities (Bouley and Kimmerer 2006; Avila and Hartman 2020) and a few fish species (Chinook Salmon smolts, *Oncorhynchus tshawytscha*; Munsch et al. 2019; Yanagitsuru et al. 2021), and warming temperatures are expected to further reduce the growth window of fishes like Delta Smelt (Brown et al. 2016). However, a declining food base for pelagic fishes, in part from the invasion of non-native taxa (e.g., *Potamocorbula amurensis*, *Corbicula fluminea*; Feyrer et al. 2003; Greene et al. 2011; Lucas and Thompson 2012), may exacerbate the shrinking effects of a warmer climate in the upper estuary as found for other ectothermic communities (Crozier et al. 2010; Cross et al. 2015; O'Gorman et al. 2016; Nelson et al. 2017). Further effort to identify the extent to which contemporary patterns of warming thermal conditions (see Bashevkin et al. 2022; Bashevkin and Mahardja 2022) have affected the size and productivity of ectotherms may provide valuable insight into how to anticipate and ameliorate climate change effects on the aquatic ectothermic community of the upper estuary.

CONCLUSION

The goal of this study was to develop temperature projections for the upper estuary using ten global climate models from the CASCaDE2 project (Brown et al. 2016) using two RCP scenarios (4.5 and 8.5). We examined effects of projected temperature increases on Delta Smelt to demonstrate how a warming climate may affect habitat needs of a fish species with significant management implications in California. However, multiple taxa of conservation interest use the upper estuary (e.g., winter run Chinook Salmon; Longfin Smelt, *Spirinchus thaleichthys*)

and are anticipated to be negatively affected by a changing climate (Yates et al. 2008; Cloern et al. 2011; Yanagitsuru et al. 2021). Consequently, using projected temperatures from this study and applying similar thermal-regime approaches specific to the life-history and physiological limitations for species of conservation interest could help resource managers anticipate future risks and inform the development of remediation strategies.

ACKNOWLEDGMENTS

Funding was provided by the Delta Stewardship Council (DSC #19125). This manuscript We thank Karen Thorne and two anonymous reviewers for helpful comments on early drafts of this manuscript. All data used in this study can be found in ScienceBase (Wulff et al. 2021). This journal article has been peer reviewed and approved for publication consistent with USGS Fundamental Science Practices (*https://pubs.usgs.gov/circ/1367/*). Any use of trade, firm, or product names is for descriptive purposes only and does not imply endorsement by the US Government.

REFERENCES

Arismendi I, Johnson S, Dunham J, Haggerty R. 2013. Descriptors of natural thermal regimes in streams and their responsiveness to change in the Pacific Northwest of North America. Freshw Biol. [accessed 2022 Jan 11];58:880–894. *https://doi.org/10.1111/fwb.12094*

Armstrong JB, Schindler DE. 2013. Going with the flow: spatial distributions of juvenile Coho Salmon track an annually shifting mosaic of water temperature. Ecosystems. [accessed 2017 Jul 5];16:1429–1441. *https://doi.org/10.2307/43677534*

Avila M, Hartman R. 2020. San Francisco Estuary mysid abundance in the fall, and the potential for competitive advantage of *Hyperacanthomysis longirostris* over *Neomysis mercedis*. Calif Fish Game. [accessed 2022 Feb 17];106:19–38.

Bashevkin SM, Mahardja B. 2022. Seasonally variable relationships between surface water temperature and inflow in the upper San Francisco Estuary. Limnol Oceanogr. [accessed 2022 Apr 13];67:684–702. *https://doi.org/10.1002/lno.12027*

Bashevkin SM, Mahardja B, Brown LR, Program DS, Council DS, States U, Survey G. 2022. Warming in the upper San Francisco Estuary: patterns of water temperature change from 5 decades of data. Limnol Oceanogr. [accessed 2022 Jan 11];1–16. *https://doi.org/10.1002/lno.12057*

Bennett WA. 2005. Critical assessment of the Delta Smelt population in the San Francisco Estuary, California. San Franc Estuary Watershed Sci. [accessed 2022 May 4];3. *https://doi.org/10.15447/sfews.2005v3iss2art*

Bouley P, Kimmerer WJ. 2006. Ecology of a highly abundant, introduced cyclopoid copepod in a temperate estuary. Mar Ecol Prog Ser. [accessed 2022 Feb 17];324:219–228. *https://doi.org/10.3354/meps324219*

Brown JH, Gillooly JF, Allen AP, Savage VM, West GB. 2004. Toward a metabolic theory of ecology. Ecology. [accessed 2017 July 16];85:1771–1789. *https://doi.org/10.1890/03-9000*

Brown LR, Bennett WA, Wagner RW, Morgan–King T, Knowles N, Feyrer F, Schoellhamer DH, Stacey MT, Dettinger M. 2013. Implications for future survival of Delta Smelt from four climate change scenarios for the Sacramento–San Joaquin Delta, California. Estuaries Coasts. [accessed 2022 Jan 11];36:754–774. *https://doi.org/10.1007/s12237-013-9585-4*

Brown LR, Komoroske LM, Wagner RW, Morgan–King T, May T, Connon RE, Fangue NA. 2016. Coupled downscaled climate models and ecophysiological metrics forecast habitat compression for an endangered estuarine fish. PLoS One. [accessed 2022 Jan 11];11:e0146724. *https://doi.org/10.1371/journal.pone.0146724*

Bush E, Herbold B, Brown LR. 2022. General conceptual model for climate change in the upper San Francisco Estuary. Sacramento (CA): Interagency Ecological Program. IEP Technical Report 99-1. [accessed 2022 Feb 17]. *https://doi.org/10.15447/sfews.2022v20iss2art1*

[CDWR] California Department of Water Resources. 2020. California Irrigation Management Information System (CIMIS). [accessed 2020 Oct 20]. Available from: https://cimis.water.ca.gov/

Cayan DR, Maurer EP, Dettinger MD, Tyree M, Hayhoe K. 2008. Climate change scenarios for the California region. Climatic Change. [accessed 2022 Apr 22];87:21–42. https://doi.org/10.1007/s10584-007-9377-6

Cloern JE, Knowles N, Brown LR, Cayan D, Dettinger MD, Tara L, Schoellhamer DH, Stacey MT, Wegen M Van Der, Wagner RW, et al. 2011. Projected evolution of California's San Francisco Bay–Delta–River system in a century of climate change. PLoS One. [accessed 2022 Jan 11];6:e24465. https://doi.org/10.1371/journal.pone.0024465

[CNDDB] California Natural Diversity Database. 2023. October 2023. State and federally listed endangered and threatened animals of California. Sacramento (CA): California Department of Fish and Wildlife. [accessed 2023 Nov 09]; 37 p. Available from: https://wildlife.ca.gov/Conservation/CESA

Cross WF, Hood JM, Benstead JP, Huryn AD, Nelson D. 2015. Interactions between temperature and nutrients across levels of ecological organization. Glob Change Biol. [accessed 2022 Jan 11];21:1025–1040. https://doi.org/10.1111/gcb.12809

Crozier LG, Zabel RW, Hockersmith EE, Achord S. 2010. Interacting effects of density and temperature on body size in multiple populations of Chinook Salmon. J Anim Ecol. [accessed 2016 Feb 1];79:342–349. https://doi.org/10.1111/j.1365-2656.2009.01641.x

Damon L, Slater S, Baxter R, Fujimura R. 2016. Fecundity and reproductive potential of wild female Delta Smelt in the upper San Francisco Estuary, California. Calif Fish Game. [accessed 2023 Sep 28];102:188–210.

Daufresne M, Lengfellner K, Sommer U. 2009. Global warming benefits the small in aquatic ecosystems. Proc Natl Acad Sci. [accessed 2020 May 15];106:12788–12793. https://doi.org/10.1073/pnas.0902080106

Davis BE, Cocherell DE, Sommer T, Baxter RD, Hung T–C, Todgham AE, Fangue NA. 2019. Sensitivities of an endemic, endangered California smelt and two non-native fishes to serial increases in temperature and salinity: implications for shifting community structure with climate change. Conserv Physiol. [accessed 2020 Mar 20];7:1–16. https://doi.org/10.1093/conphys/coy076

Feyrer F, Herbold B, Matern SA, Moyle PB. 2003. Dietary shifts in a stressed fish assemblage: consequences of a bivalve invasion in the San Francisco Estuary. Environ Biol Fishes. [accessed 2022 Feb 17];67:277–288. https://doi.org/10.1023/A:1025839132274

Ghalambor C, Gross E, Grosholz E, Jeffries K, Largier J, McCormick S, Sommer T, Velotta J, Whitehead A. 2021. Ecological effects of climate-driven salinity variation in the San Francisco Estuary: can we anticipate and manage the coming changes? San Franc Estuary Watershed Sci. [accessed 2023 Sep 28];19. https://doi.org/10.15447/sfews.2021v19iss2art3

Goertler P, Mahardja B, Sommer T. 2021. Striped Bass (*Morone saxatilis*) migration timing driven by estuary outflow and sea surface temperature in the San Francisco Bay–Delta, California. Sci Rep. [accessed 2022 Feb 17];11:1–11. https://doi.org/10.1038/s41598-020-80517-5

Greene VE, Sullivan LJ, Thompson JK, KimmererWJ. 2011. Grazing impact of the invasive clam *Corbula amurensis* on the microplankton assemblage of the northern San Francisco Estuary. Mar Ecol Prog Ser. [accessed 2022 Feb 17];431:183–193. https://doi.org/10.3354/meps09099

Herbold B, Bush E, Castillo G, Colombano D, Hartman R, Lehman P, Mahardja B, Sommer T. 2022. Climate change impacts on San Francisco Estuary aquatic ecosystems: a review. San Franc Estuary Watershed Sci. [accessed 2022 Aug 11];20(2). https://doi.org/10.15447/sfews.2022v20iss2art1

Hobbs JA, Lewis LS, Willmes M, Denney C, Bush E. 2019. Complex life histories discovered in a critically endangered fish. Sci Rep. [accessed 2019 Nov 16];9:1–12. https://doi.org/10.1038/s41598-019-52273-8

Hung T, Hammock B, Sandford M, Stillway M, Park M, Lindberg J, Teh S. 2022. Temperature and salinity preferences of endangered Delta Smelt (*Hypomesus transpacificus*, *Actinopterygii*, *Osmeridae*). Sci Rep. [accessed 2023 Sep 28];12:16558. *https://doi.org/10.1038/s41598-022-20934-w*

Isaak DJ, Luce CH, Horan DL, Chandler GL, Wollrab SP, Dubois WB, Nagel DE. 2020. Thermal regimes of perennial rivers and streams in the western United States. J Am Water Resour Assoc. [accessed 2021 Dec 19];56:842–867. *https://doi.org/10.1111/1752-1688.12864*

Jeffries KM, Connon RE, Davis BE, Komoroske LM, Britton MT, Sommer T, Todgham AE, Fangue NA. 2016. Effects of high temperatures on threatened estuarine fishes during periods of extreme drought. J Exp Biol. [accessed 2022 Jan 11];219:1705–1716. *https://doi.org/10.1242/jeb.134528*

Kammerer B, Hung T, Baxter R, Teh S. 2016. Physiological effects of salinity on Delta Smelt, *Hypomesus transpacificus*. Fish Physiol Biochem. [accessed 2023 Sep 28];42:219–232. *https://doi.org/10.1007/s10695-015-0131-0*

Kimmerer WJ. 2004. Open water processes of the San Francisco Estuary: from physical forcing to biological responses. San Franc Estuary Watershed Sci. [accessed 2022 Oct 15];2(1). *https://doi.org/10.15447/sfews.2004v2iss1art1*

Knowles N, Pierce DW, Cayan DR. 2018. Responses of unimpaired flows, storage, and managed flows to scenarios of climate change in the San Francisco Bay–Delta watershed. Water Resour Res. [accessed 2022 Jan 11];54:7631–7650. *https://doi.org/10.1029/2018WR022852*

Komoroske L, Connon R, Lindberg J, Cheng B, Castillo G, Hasenbein M, Fangue N. 2014. Ontogeny influences sensitivity to climate change stressors in an endangered fish. Conserv Physiol. [accessed 2023 Sep 28];2:cou008. *https://doi.org/10.1093/conphys/cou008*

Livneh B, Bohn TJ, Pierce DW, Munoz–Arriola F, Nijssen B, Vose R, Cayan DR, Brekke L. 2015. A spatially comprehensive, hydrometeorological data set for Mexico, the US, and southern Canada 1950–2013. Sci Data. [accessed 2022 May 4];2:1–12. *https://doi.org/10.1038/sdata.2015.42*

Lucas L, Thompson J. 2012. Changing restoration rules: exotic bivalves interact with residence time and depth to control phytoplankton productivity. Ecosphere. [accessed 2023 Sep 28];3:1–26. *https://doi.org/10.1890/ES12-00251.1*

Maheu A, Poff NL, St-Hilaire A. 2016. A classification of stream water temperature regimes in the conterminous USA. River Res Appl. [accessed 2022 Jan 11];32:896–906. *https://doi.org/10.1002/rra.2906*

Merz J, Hamilton S, Bergman P, Cavallo B. 2011. Spatial perspective for Delta Smelt: a summary of contemporary survey data. Calif Fish Game. [accessed 2023 Nov 09];97(4):164–189. Available from: *https://nrm.dfg.ca.gov/FileHandler.ashx?DocumentID=46489&inline=1*

Merz JE, Bergman PS, Simonis JL, Delaney D, Pierson J, Anders P. 2016. Long-term seasonal trends in the prey community of Delta Smelt (*Hypomesus transpacificus*) within the Sacramento–San Joaquin Delta, California. Estuaries Coasts. [accessed 2022 Feb 17];39:1526–1536. *https://doi.org/10.1007/s12237-016-0097-x*

Moyle PB, Brown LR, Durand JR, Hobbs JA. 2016. Delta Smelt: life history and decline of a once-abundant species in the San Francisco Estuary. San Franc Estuary Watershed Sci. [accessed 2022 Oct 5];14. *https://doi.org/doi.org/10.15447/sfews.2016v14iss2art6*

Munsch S, Greene C, Johnson R, Satterthwaite W, Imaki H, Brandes P. 2019. Warm, dry winters truncate timing and size distribution of seaward-migrating salmon across a large, regulated watershed. Ecol Appl. [accessed 2022 Jan 11];29:e01880. *https://doi.org/10.1002/eap.1880*

Nelson D, Benstead JP, Huryn AD, Cross WF, Hood JM, Johnson PW, Junker JR, Gíslason GM, Ólafsson JS. 2017. Experimental whole-stream warming alters community size structure. Glob Change Biol. [accessed 2022 Feb 17];23:2618–2628. *https://doi.org/10.1111/gcb.13574*

O'Gorman EJ, Ólafsson ÓP, Demars BOL, Friberg N, Guðbergsson G, Hannesdóttir ER, Jackson MC, Johansson LS, McLaughlin ÓB, Ólafsson JS, et al. 2016. Temperature effects on fish production across a natural thermal gradient. Glob Change Biol. [accessed 2021 Jan 11];22:3206–3220. *https://doi.org/10.1111/gcb.13233*

Oksanen J, Blanchet FG, Friendly M, Kindt R, Legendre P, McGlinn D, Minchin PR, O'Hara RB, Simpson GL, Solymos P, et al. 2020. vegan: Community Ecology Package. [accessed 2022 Jan 11]. *https://CRAN.R-project.org/package=vegan*

Olden JD, Naiman RJ. 2010. Incorporating thermal regimes into environmental flows assessments: modifying dam operations to restore freshwater ecosystem integrity. Freshw Biol. [accessed 2022 Apr 13];55:86–107. *https://doi.org/10.1111/j.1365-2427.2009.02179.x*

Palmer MA, Lettenmaier DP, Poff NL, Postel SL, Richter B. 2009. Climate change and river ecosystems: protection and adaptation options. Environ Manage. [accessed 2022 Jan 11];44:1053–1068. *https://doi.org/10.1007/s00267-009-9329-1*

Pierce DW, Cayan DR, Thrasher BL. 2014. Statistical downscaling using localized constructed analogs (LOCA). J Hydrometeorology. [accessed 2022 Feb 17];15(6), 2558–2585. *http://journals.ametsoc.org/doi/abs/10.1175/JHM-D-14-0082.1*

Pohlert T. 2020. trend: non-parametric trend tests and changepoint detection. R package ver. 1.1. 2. [accessed 2022 Oct 5]. *https://CRAN.R-project.org/package=trend*

R Core Team. 2021. R: a language and environment for statistical computing. [accessed 2022 Jan 11]. *https://www.R-project.org/*

Sacramento–San Joaquin Delta Reform Act, California Water Code § 85304 (2009). Chapter 3 (amended April 26, 2018): a more reliable water for California. [accessed 2023 Sep 28]. Available from: *https://deltacouncil.ca.gov/pdf/delta-plan/2018-04-26-amended-chapter-3.pdf*

Sen PK. 1968. Estimates of the regression coefficient based on Kendall's tau. J Am Stat Assoc. [accessed 2022 Oct 5];63:1379–1389. *https://doi.org/10.1080/01621459.1968.10480934*

Sherbakov T, Malig B, Guirguis K, Gershunov A, Basu R. 2018. Ambient temperature and added heat wave effects on hospitalizations in California from 1999 to 2009. Environ Res. [accessed 2022 May 4];160:83–90. *https://doi.org/10.1016/j.envres.2017.08.052*

Sheridan JA, Bickford D. 2011. Shrinking body size as an ecological response to climate change. Nat Climate Change. [accessed 2022 Jan 11];1:401–406. *https://doi.org/10.1038/nclimate1259*

Sommer T, Mejia FH, Nobriga ML, Feyrer F, Grimaldo L. 2011. The spawning migration of Delta Smelt in the upper San Francisco estuary. San Franc Estuary Watershed Sci. [accessed 2023 Nov 9];9:2. *http://dx.doi.org/10.15447/sfews.2011v9iss2art2*

Stern MA, Flint LE, Wright SA. 2020. The future of sediment transport and streamflow under a changing climate and the implications for long-term resilience of the San Francisco Bay–Delta. Water Resour Res. [accessed 2022 Jan 11];56:e2019WR026245. *https://doi.org/10.1029/2019WR026245*

Vroom J, van der Wegen M, Martyr–Koller RC, Lucas LV. 2017. What determines water temperature dynamics in the San Francisco Bay–Delta system. Water Resour Res. [accessed 2022 Jan 11];53:9901–9921. *https://doi.org/10.1002/2016WR020062*

Wagner RW, Stacey M, Brown LR, Dettinger M. 2011. Statistical models of temperature in the Sacramento–San Joaquin Delta under climate-change scenarios and ecological implications. Estuaries Coasts. [accessed 2022 Jan 11];34:544–556. *https://doi.org/10.1007/s12237-010-9369-z*

Wulff ML, Brown LR, Huntsman BM, Knowles N, Wagner W. 2021. Data used in projected air and water temperatures for selected regions of the upper San Francisco Estuary and Yolo Bypass under 20 scenarios of climate change. USGS ScienceBase-Catalog. [accessed 2022 Feb 17]. *https://doi.org/10.5066/P9CXGU44*

Yanagitsuru YR, Main MA, Lewis LS, Hobbs JA, Hung T, Connon RE, Fangue NA. 2021. Effects of temperature on hatching and growth performance of embryos and yolk-sac larvae of a threatened estuarine fish: Longfin Smelt (*Spirinchus thaleichthys*). Aquaculture. [accessed 2022 Jan 11];537:736502. *https://doi.org/10.1016/j.aquaculture.2021.736502*

Yates D, Galbraith H, Purkey D, Huber–Lee A, Sieber J, West J, Herrod–Julius S, Joyce B. 2008. Climate warming, water storage, and Chinook Salmon in California's Sacramento Valley. Climatic Change. [accessed 2022 May 4];91:335–350. *https://doi.org/10.1007/s10584-008-9427-8*